Doubly Differential Final-State Momentum Distributions of the Ionization Products in Collision of Bare Ions with Hydrogen

Lokesh C. Tribedi,[1,*] P. Richard,[1] Y. D. Wang,[1] C. D. Lin,[1] and R. E. Olson[2]
[1]*J.R. Macdonald Laboratory, Department of Physics, Kansas State University, Manhattan, Kansas 66506-2601*
[2]*Physics Department, University of Missouri-Rolla, Rolla, Missouri 65401*
(Received 21 February 1996; revised manuscript received 19 August 1996)

In this paper recoil-ion production cross sections are presented differential in recoil-ion longitudinal momentum and electron emission angle in ionization of atomic and molecular hydrogen by bare ion projectiles. A new formulation for constructing these double differential distributions from the measured electron double differential cross sections is used. A novel feature is the separation of two different branches of the recoil-ion longitudinal momentum distribution corresponding to soft and hard collision mechanisms of ionization. The single differential distributions have also been derived. [S0031-9007(96)01510-4]

PACS numbers: 34.50.Fa, 39.30.+w

Ionization in ion-atom collisions is a fundamental process which is important in understanding three-body dynamics. The precise measurement of electron double differential cross sections (DDCS) in electron energy and angle has enriched our understanding of the different ionization mechanisms for soft electron emission, binary encounter (BE) electron emission, and the electron capture to the continuum cusp production. While the ejected electron spectroscopy (EES) has been a subject of extensive study in the past two decades [1–7], the recoil-ion momentum spectroscopy (RIMS) has been developed only recently [8–13]. The RIMS has provided valuable information on the various ionization mechanisms such as electron-electron, electron-nucleus, and postcollision interactions via the measurements of the cross sections differential in recoil-ion (p_R) and electron momenta (p_e). In a kinematically complete experiment on ionization, Moshammer *et al.* [10] have measured the single differential cross sections ($d\sigma/dp_{R\parallel}$ and $d\sigma/dp_{e\parallel}$) using high resolution RIMS technique.

The connection and the complementary nature between the EES and RIMS techniques have not been fully explored. It is shown here that the EES measurements, although not kinematically complete, can be used to derive a variety of doubly differential cross sections with respect to electron emission angle (θ_e) and the longitudinal momenta the electron ($p_{e\parallel}$), recoil-ion ($p_{R\parallel}$), and the projectile longitudinal momentum transfer ($p_{P\parallel}$). The doubly differential recoil-ion momentum distributions can provide a deeper understanding of the three-body and binary collision mechanisms for ionization. In fact, the soft and hard collisions can be separated as two different branches with widely different cross sections. Moreover, the high resolution RIMS experiments need to use a cold jet as the target. Building of a cold jet for atomic and molecular hydrogen still remains a challenging task, and hence the conventional RIMS technique, as it stands today, cannot approach these targets. The present technique will thus be extremely useful and unique in providing knowledge on the final-state momentum distributions of the primary collision products of ionization in the fundamental collision system, namely, $H^+ + H$, and also in ionization of the simplest molecule H_2 by fast bare ions.

To manifest the present method we derive here the doubly differential longitudinal momentum distributions for the recoil ions and the electrons in ionization of hydrogen for two different collision systems: (i) bare carbon ions (2.5 MeV/u, $v = 10$ a.u.) colliding with molecular hydrogen and (ii) low energy (0.114 MeV/u, $v = 2.14$ a.u.) protons colliding with atomic hydrogen. These results are derived from the electron DDCS data measured recently [7,14] using standard EES techniques and will not be discussed here. The same electron spectrometer (with an energy resolution of about 5%) was used in both measurements, and the electrons emitted in ionization of H and H_2 were detected at ten [7] and twelve [14] different angles between 15° and 165°.

In Fig. 1(a), we show the electron DDCS ($\frac{d^2\sigma}{d\varepsilon_e d\Omega_e}$) spectra [14] as a function of electron energy (ε_e), for $\theta_e = 45°$ and $\theta_e = 160°$ for 2.5 MeV/u $C^{6+} + H_2$. These data sets will be used below for the present analysis. Our calculations using the continuum distorted wave-eikonal initial state (CDW-EIS) approximation [15,16] are also shown in Fig. 1. These calculations are based on an independent electron approximation, as explained in Ref. [14].

The final-state electron longitudinal momentum distribution in terms of electron DDCS can be expressed as

$$\frac{d^2\sigma}{dp_{e\parallel}d\Omega_e} = \frac{|p_{e\parallel}|}{\cos^2\theta_e}\,\frac{d^2\sigma}{d\varepsilon_e d\Omega_e}\,. \tag{1}$$

The fundamental law of energy-momentum conservation plays the key role in obtaining the recoil-ion longitudinal momentum distributions from the EES spectrum. The key equation governing the energy and longitudinal

 © 1996 The American Physical Society

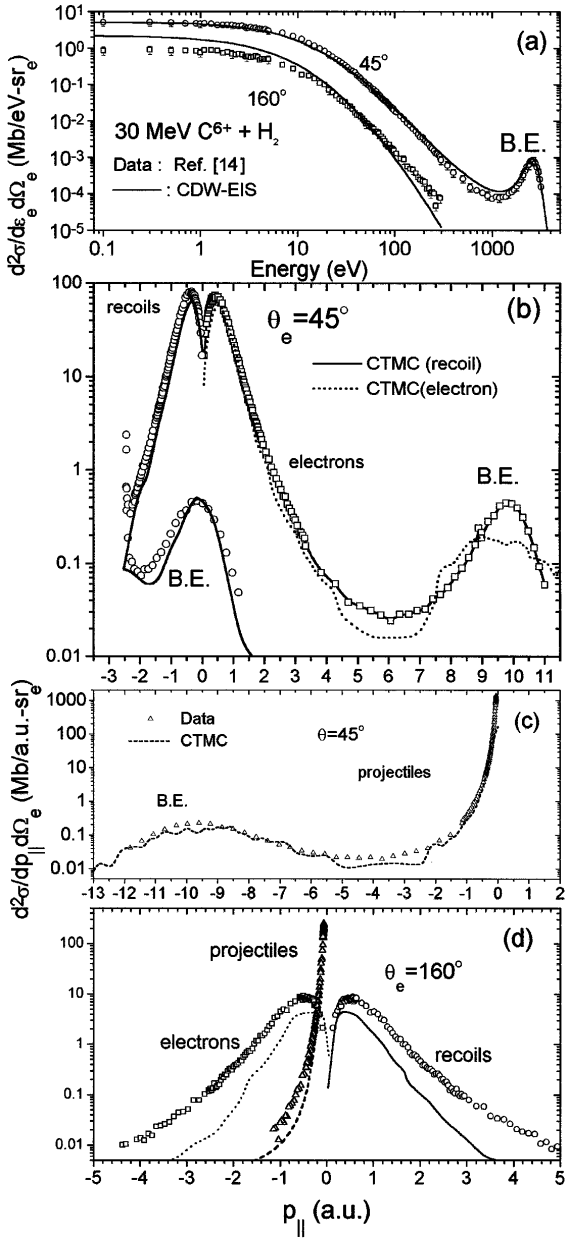

FIG. 1. (a) Electron doubly differential cross sections for $\theta_e = 45°$ and 160° in ionization of H_2 by 30 MeV C^{6+} taken from Ref. [14] and CDW-EIS calculation. (b) Doubly differential longitudinal momentum distributions of electrons (squares) and recoil ions (circles) for $\theta_e = 45°$ derived from electron DDCS. CTMC calculations are also shown. (c) The projectile longitudinal momentum transfer distribution along with CTMC calculations. (d) Similar distributions for $\theta_e = 160°$ and CTMC calculations. The symbols have the same meanings as in (b) and (c).

momentum conservation can be expressed as

$$-p_{P\|} = p_{e\|} + p_{R\|} \approx -Q/v = (\varepsilon_e - \varepsilon_i)/v\,, \quad (2)$$

where $p_{P\|}$ refers to the longitudinal momentum transfer of the projectile with initial velocity v, and $|\varepsilon_i|$ is the binding energy of the target atom in the initial state. The quantity Q refers to the Q-value of the reaction. From Eq. (2), recoil-ion longitudinal momentum can be expressed as

$$p_{R\|} = (\varepsilon_e - \varepsilon_i)/v - \sqrt{2\varepsilon_e}\cos\theta_e\,. \quad (3)$$

This relation is valid for a three-body system involving a heavy projectile which suffers small energy loss compared to its initial energy and is correct to the order of m_e/m_P and m_e/m_T, where m_e, m_P, and m_T represent the mass of electron, projectile, and target. The recoiling particle can be uniquely defined only in collisions of bare ions with atomic hydrogen. In the case of other targets (such as H_2/He), Eq. (3) merely reflects the momentum balance in the center of the mass frame, and therefore the recoil momentum refers to the momentum of the "compound" third party which is separable from the ionized electron and the projectile. Furthermore, for the present collision system ($C^{6+} + H_2$) the cross sections for dissociative and double ionization are estimated to be about 5% to 7% and 3% of the total ionization cross section, respectively. These estimations are based on the previous works [17–19] on similar collision systems and from recent experiments [20]. Therefore, the most probable recoil ion would be the H_2^+, in the present case.

The DDCS, with respect to $p_{R\|}$ and θ_e, can be obtained from the following transformation:

$$\frac{d^2\sigma}{dp_{R\|}d\Omega_e} = \left|\frac{1}{(1/v) - (\cos\theta_e/\sqrt{2\varepsilon_e})}\right| \frac{d^2\sigma}{d\varepsilon_e d\Omega_e}\,. \quad (4)$$

Such doubly differential measurements can be carried out by detecting the recoil ions in coincidence with the ejected electrons emitted in a given direction. No such measurements have been reported. Similarly, the projectile momentum transfer distribution can also be given by

$$\frac{d^2\sigma}{dp_{P\|}d\Omega_e} = v\,\frac{d^2\sigma}{d\varepsilon_e d\Omega_e}\,. \quad (5)$$

The DDCS in ε_e and the projectile scattering angle have been measured recently [21] for low energy p + He.

In Fig. 1(b) we present $\frac{d^2\sigma}{dp_{e\|}d\Omega_e}$ and $\frac{d^2\sigma}{dp_{R\|}d\Omega_e}$ for $\theta_e = 45°$ for $C^{6+} + H_2$. The peak at 0.43 a.u. in the electron momentum distribution consists mainly of the low energy ($\varepsilon_e \approx 0.2$ a.u.) electrons arising from the soft collisions. Another wide peak at about 10 a.u. is due to the hard BE collisions. The recoil-ion momentum distribution, on the other hand, has a few features. First, we note that there is a divergence in this distribution (at $p_{R\|} = -2.44$ a.u.) arising because of the vanishing denominator in Eq. (4) for $p_e = v\cos\theta_e$. Second, there are two branches in this distribution which can be explained from Eq. (3). This equation can be solved for $\varepsilon_e(p_{R\|}, \theta_e)$ [22,23], and it can be shown that $\varepsilon_e(p_{R\|}, \theta_e)$ is a double-valued function of $p_{R\|}$ for a given θ for $p_{R\|} < |\varepsilon_i|/v$. The upper branch of the recoil-ion distribution corresponds to low energy electrons for $\varepsilon_e \leq \frac{1}{2}v^2\cos^2\theta_e$. The peak in the upper branch near

$p_{R\|} = -0.35$ a.u. is associated with the soft collision electron peak (at $p_{e\|} = 0.43$ a.u.). The lower branch is composed of emitted recoil ions associated with the higher energy ($\varepsilon_e \geq \frac{1}{2}v^2 \cos^2\theta_e$) part of the electron spectrum. The wide peak in this lower branch corresponds to the BE process. This distribution peaks near $p_{R\|} \approx 0$, signifying that this process involves primarily the collision between the electron and the projectile. The projectile longitudinal momentum transfer distribution [Fig. 1(c)] starts at -0.057 a.u., which is the minimum momentum transfer ($|\varepsilon_i|/v$) required to ionize H_2 and falls off rapidly, indicating that most of the cross sections for projectile momentum transfer are related to the very low energy electron emission. However, there is a well separated wide peak in this distribution due to the BE process at about -10 a.u., satisfying the longitudinal momentum balance [Eq. (2)] since $p_{e\|}^{\mathrm{BE}} \approx +10$ a.u. and $p_{R\|}^{\mathrm{BE}} \approx 0$ a.u.

Classical trajectory Monte Carlo (CTMC) calculations were performed and show an excellent agreement with the electron, projectile, and recoil-ion longitudinal momentum distributions [Figs. 1(b) and 1(c)]. The two branches in the recoil-ion distributions could be obtained from the CTMC calculations by identifying the collisions producing low and high energy ($\varepsilon_e \geq \frac{1}{2}v^2 \cos^2\theta_e$) electrons. The CDW-EIS calculations also give good agreement with the data (not shown). However, these results are obtained by using the same transformations [Eqs. (1)–(5)] as used for the experimental data. The CTMC calculations therefore provide an independent check on the collision dynamics since no such transformations are performed. This calculation does not yield the singularity present in the transformed data.

It may be emphasized that the upper branch ("soft branch") in the recoil-ion momentum distribution is dominated mainly by the three-body soft collision ionization mechanism, and the lower branch ("hard branch"), on the other hand, consists mostly of the two-body hard collision process, namely, the binary encounter. This is the first manifestation of the existence of two branches in recoil-ion longitudinal momentum distribution with widely different cross sections.

At the backward electron angle, $\theta_e = 160°$, the situation is reversed [Fig. 1(d)]: the electron distribution peaks near -0.57 a.u. and the recoils near $+0.65$ a.u. For this angle (and for all other backward angles), the $p_{R\|}$ (ε_e) is a single valued function of ε_e (i.e., only one branch is allowed kinematically, since $p_{R\|} > |\varepsilon_i|/v = 0.057$). The CTMC calculations, although they provide a good qualitative agreement, underestimate the data slightly.

The similar distributions for the most fundamental collision system, i.e., $H^+ + H$, are shown in Figs. 2(a) and 2(b) for $\theta_e = 15°$. This is a pure three-body collision system with H^+ being the only recoiling ions. All the features observed for the high energy collision system ($C^{6+} + H_2$), including the soft and hard branches, are also present in this case and also reproduced by the CTMC calculations.

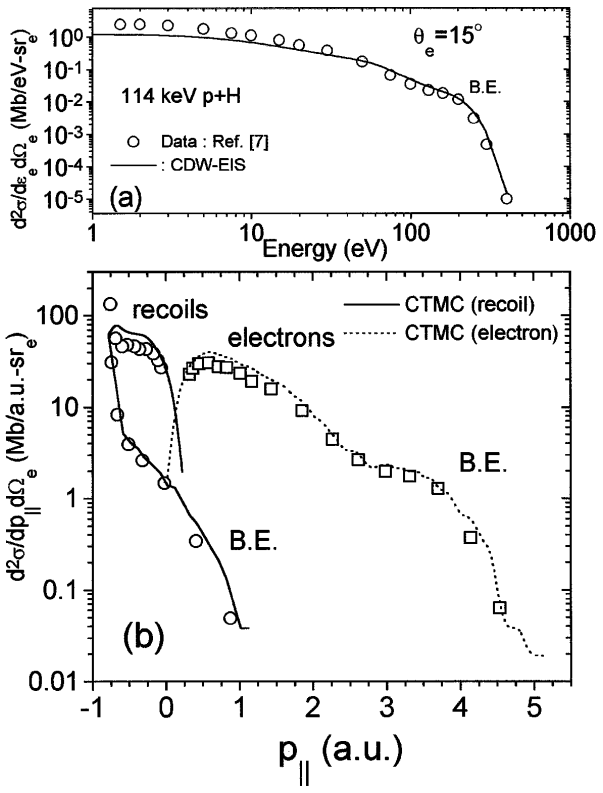

FIG. 2. (a) The electron DDCS for 114 keV p + H for $\theta_e = 15°$ (from Ref. [7]) and CDW-EIS calculation. (b) Derived doubly differential longitudinal momentum distributions of electrons (squares) and recoil ions (circles) and CTMC calculations.

Single differential longitudinal momentum distributions for the electrons ($d\sigma/dp_{e\|}$) and recoil ions ($d\sigma/dp_{R\|}$) were deduced [Figs. 3(a) and 3(b)] by integrating the double differential distributions for different emission angles (θ_e) between 15° and 165°. It was necessary to have data in small angular steps to perform the numerical integration. The contribution of the divergence (in the recoil-ion DDCS) to the single differential cross section ($d\sigma/dp_{R\|}$) is negligible since the interval $\Delta p_{R\|}$ shrinks to zero at the point of divergence. It may be noted that the electron distribution peaks near a positive longitudinal momentum ≈0.1 a.u. for $C^{6+} + H_2$ and near 0.3 a.u. for the $H^+ + H$ collision system. The larger shift in the distribution in the case of $H^+ + H$ is primarily due to the large Q/v-value (= 0.24 a.u.) as compared to the high energy collision system for which $Q/v = 0.057$ a.u. The recoil-ion distributions, for both of the collision systems, are peaked near $p_{R\|} \approx 0$, indicating that the post collision interaction in the present collision systems is much weaker than that observed for more highly charged ions [10]. No measurements on the recoil-ion momentum distributions for this fundamental collision system ($H^+ + H$) have been reported before.

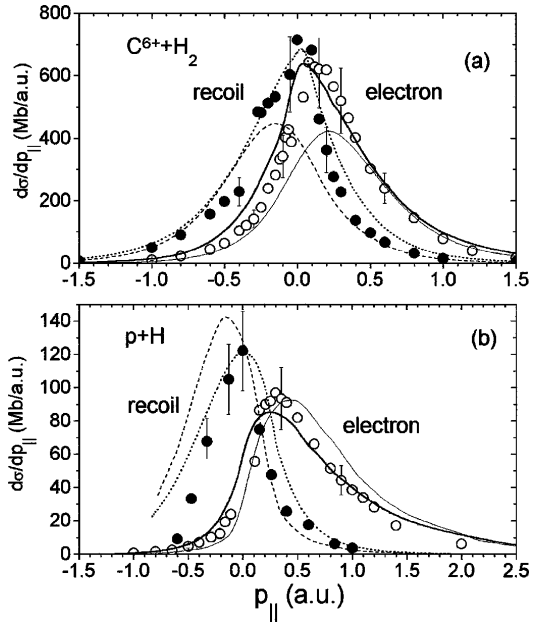

FIG. 3. The single differential longitudinal momentum distributions of electrons (open circles) and recoil ions (closed circles) for (a) 30 MeV $C^{6+} + H_2$ and (b) 114 keV $H^+ + H$. The thick solid (dotted) line is the CDW-EIS calculation for electron (recoil) distributions. The thin solid (dashed) line is the CTMC calculation for electron (recoil) distributions.

These distributions, along with the peak positions, are well reproduced by the CDW-EIS calculations for both collision systems. The CTMC calculations predict larger shifts and underestimate the cross sections for $C^{6+} + H_2$. In the case of $H^+ + H$, these calculations provide a better agreement with the data.

The transverse momentum of the recoil ion is given by $p_{RTr} = p_{PTr} - p_{eTr}$. Since p_{eTr} is the only measured quantity from the EES, it alone cannot determine the transverse momentum distribution of the recoil ion or the projectile.

In summary, we have introduced and explored the doubly differential final-state longitudinal momentum distributions of the electrons, recoil ions, and the projectiles in ion-atom ionization. The complementary nature of the electron spectroscopy and the recoil-ion momentum spectroscopy have been investigated to show that many of the important features of current RIMS experiments can be addressed from the EES measurements. The influence of the three-body ionization, as well as the binary encounter processes on the recoil-ion (and projectile) longitudinal momentum distributions, have been explored. The separation of the soft and hard collision branches of recoil-ion distributions is a novel feature of the present technique. This method of studying the recoil-ion longitudinal momentum distributions with a pure three-body collision system like $H^+ + H$ is unique since the conventional high resolution RIMS technique, which needs a cold jet target of atomic hydrogen, cannot yet approach this fundamental collision system. The present method does not require a cold jet and therefore can be applied for other ion-atom collision systems.

We would like to thank C. L. Cocke and S. Hagmann for valuable discussions and suggestions. This work is supported by the Division of Chemical Sciences, Office of Basic Energy Sciences, Office of Energy Research, U.S. Department of Energy.

*On leave from Tata Institute of Fundamental Research, Homi Bhabha Road, Bombay 400005, India.

[1] G. B. Crooks and M. E. Rudd, Phys. Rev. Lett. **25**, 1599 (1970).
[2] K. G. Harrison and M. Lucas, Phys. Lett. **33A**, 149 (1970).
[3] Steven T. Manson, L. H. Toburen, and N. Stolterfoht, Phys. Rev. A **12**, 60 (1975).
[4] M. E. Rudd, L. H. Toburen, and N. Stolterfoht, Nucl. Data Tables **18**, 413 (1976).
[5] D. H. Lee, P. Richard, T. J. M. Zouros, J. M. Sanders, J. L. Shinpaugh, and H. Hidmi, Phys. Rev. A **41**, 4816 (1990).
[6] S. Suárez, C. Garibotti, W. Meckbach, and G. Bernardi, Phys. Rev. Lett. **70**, 418 (1993).
[7] G. W. Kerby III, M. W. Gealy, Y.-Y. Hsu, and M. E. Rudd, Phys. Rev. A **51**, 2256 (1995).
[8] C. L. Cocke and R. E. Olson, Phys. Rep. **205**, 153 (1991).
[9] R. Ali, V. Frohne, C. L. Cocke, M. Stöckli, and M. Raphaeliam, Phys. Rev. Lett. **69**, 2491 (1992).
[10] R. Moshammer *et al.*, Phys. Rev. Lett. **73**, 3371 (1994).
[11] W. Wu *et al.*, Phys. Rev. Lett. **72**, 3170 (1994).
[12] R. Dörner *et al.*, Phys. Rev. Lett. **72**, 3166 (1994).
[13] R. Dörner, V. Mergel, L. Zhaoyuan, J. Ulrich, L. Spielberger, R. E. Olson, and H. Schmidt-Böcking, J. Phys. B **28**, 435 (1995).
[14] Lokesh C. Tribedi, P. Richard, Y. D. Wang, D. Ling, C. D. Lin, R. Moshammer, G. W. Kerby, and M. E. Rudd, Phys. Rev. A **54**, 2154 (1996).
[15] D. S. F. Crothers and J. F. McCann, J. Phys. B **16**, 3229 (1983).
[16] P. D. Fainstein, V. H. Ponce, and R. D. Rivarola, J. Phys. B **24**, 3091 (1991).
[17] E. Krishnakumar, Bhas Bapat, F. A. Rajgara, and M. Krishnamurthy, J. Phys. B **27**, L777 (1994).
[18] S. Cheng, C. L. Cocke, E. Y. Kamber, C. C. Hsu, and S. L. Varghese, Phys. Rev. A **42**, 214 (1990).
[19] E. Krishnakumar and F. A. Rajgara, J. Phys. B **26**, 4155 (1993).
[20] A. Landers and C. L. Cocke *et al.* (private communication). The time of flight spectrum of the recoil ions for 30 MeV $C^{6+} + H_2$ is measured by these authors. The preliminary results agree approximately with the estimation for the ratio of double + dissociative ionization to the total ionization.
[21] T. Vajnai, A. D. Gaus, J. A. Brand, W. Htwe, D. H. Madison, R. E. Olson, J. L. Peacher, and M. Schulz, Phys. Rev. Lett. **74**, 3588 (1995).
[22] Y. D. Wang, Lokesh C. Tribedi, P. Richard, C. L. Cocke, V. D. Rodríguez, and C. D. Lin, J. Phys. B **29**, L203 (1996).
[23] V. D. Rodríguez, Y. D. Wang, and C. D. Lin, Phys. Rev. A **52**, 9 (1995).